Self-avoiding Lévy flights at upper marginal dimensions

Jangnyeol Moon and Hisao Nakanishi
Department of Physics, Purdue University, West Lafayette, Indiana 47907
(Received 31 January 1989)

We study the node-avoiding (NALF) and path-avoiding extensions of the Lévy flights in terms of the critical exponents ν and γ and the leading corrections to scaling, using Monte Carlo simulations with enrichment as the main technique. We focus on the upper marginal dimensions of NALF as predicted by the magnetic analogy where the renormalization-group results should be quantitatively exact for NALF if the method is valid at all. Similarly, we also focus on the boundary between the long-range and short-range behavior of NALF above four dimensions where the renormalization results should again be exact. Thus we investigate the self-avoiding Lévy flights on hypercubic lattices from $d=2$ to 6 dimensions and obtain behavior consistent with logarithmic corrections to scaling in the moments of their end-to-end distance distributions. In addition, the effective Lévy index μ_{eff} is determined from the logarithmic averages of individual step sizes and compared for the two self-avoiding extensions.

I. INTRODUCTION

Previously, two self-avoiding extensions were proposed[1] in order to add excluded-volume effects to the original random Lévy flights of Mandelbrot.[2] The random Lévy flights are the nonexcluded-volume random walks with a variable step size whose probability distribution is a power law

$$P(l) \propto l^{-\mu-1} , \tag{1}$$

where $\mu > 0$ is called the Lévy index. The two extensions are termed node-avoiding (NALF) and path-avoiding (PALF) Lévy flights, where the former do not visit the same site on a lattice more than once and the latter additionally do not intersect themselves. These self-avoiding walks are still characterized by the Lévy index μ, but the actual step sizes are determined algorithmically by removing forbidden configurations from the ensemble of the *random* Lévy flights, and thus, in the final ensemble, they are not in general distributed as in (1) with the nominal index μ but perhaps rather with an effective index μ_{eff}.

In the off-lattice continuum, the former could be interpreted to describe a chain of negligible cross sections except at turns where a finite-size *bead* is present; the latter could describe, for example, a polymeric chain with the excluded volume comparable to the monomer size throughout its length.

The greatest motivation for our study is the intrinsic interest in the complex structures of these walks. In particular, we wish to study if the idea of asymptotic scale invariance is applicable and the associated results of renormalization-group calculations are correct. We wish to also find, e.g., how the *fractal* dimension is related to μ_{eff}, if they are indeed scale invariant. Ultimately, we would like to contribute to relating step-size distributions to the overall conformation for non-Markovian walks in general.

However, the subject is not devoid of more practical applications. Thus these problems are potentially relevant to the statistics of various polymers whose persistence length is broadly distributed. This might occur, for example, when they are embedded in a medium which is itself scale invariant or critical, that in turn imposes a broad distribution of length scales on the polymers. The case of a critical (or *fractal)* medium may apply also to certain transport or networking problems as well. The NALF extension was also discussed[3] in relation to the problem of polymer adsorption onto a solid surface.

The relationship between the two variants—the NALF and the PALF—is not obvious and has been the subject of some controversy.[4,5] If μ is so large that both flights are essentially like the usual short-range self-avoiding walk (SAW), then they must obviously behave in the same way. Also, if there exists a minimum value μ_1 below which both behave as classical Lévy flights, then they should behave in the same way for $\mu < \mu_1$. It seems intuitively obvious that they should behave in the same way for sufficiently large spatial dimensionality d as well. However, for general values of μ and d, it is far from clear whether they belong to the same universality class.[6] Indeed, for $d=1$, analytic and numerical studies[4] indicated that they have different asymptotic behavior for $\frac{1}{2} \le \mu \le 1$. Not only different, but surprisingly the NALF with less excluded volume turned out to be larger than the PALF for $d=1$. The latter result is one of the reasons why the intrinsic structures of these walks are subjects of interest.

In this paper we mainly study the two critical exponents ν and γ for the asymptotic behavior for large number of steps N. The exponent ν is defined by the end-to-end distance $\langle R_N^x \rangle^{1/x}$ for sufficiently small $x > 0$ as

$$\langle R_N^x \rangle^{1/x} \sim A N^{\nu} , \tag{2}$$

while γ is defined by the weighted number of N-step flights G_N as

$$G_N \sim z_{\text{eff}}^N N^{\gamma-1} , \tag{3}$$

where each walk is weighted by the product of the probabilities for the individual steps in the walk and z_{eff} is the effective coordination number of the lattice available to the walk. This is a proper extension of the total number of walks whose step sizes are fixed, as can be verified very easily.

In this work we restrict our attention mostly to the values of d and μ which satisfy either

$$d=2\mu \quad (1 \le d \le 4) , \tag{4}$$

or

$$d \ge 4, \quad \mu=2 , \tag{5}$$

or

$$d=4, \quad \mu \ge 2 . \tag{6}$$

These points are sketched in Fig. 1, which also shows the division of the parameter space (d,μ) into four qualitatively different regions. Equation (4) corresponds to the upper marginal dimensions for the NALF according to the extensions[1] to $n \to 0$ of the renormalization-group predictions[7] of the long-range n-vector-model[6] spin Hamiltonian. Equation (5), on the other hand, corresponds to the boundary for the NALF between classical Lévy behavior and ordinary (short-range) random-walk behavior, and Eq. (6) corresponds to the boundary between the SAW and random-walk behaviors of the NALF. We restrict this study mostly to these points because the results of renormalization-group theory for the NALF must be exact there if the method is valid and because it allows us to concentrate on a manageably small parameter space to explore. In addition, the asymptotic behavior of the random Lévy flights at $\mu=2$ is known exactly.[8]

In Sec. II, known theoretical results are reviewed and some additional results are given. Section III gives the results of our Monte Carlo calculations for the exponents ν and γ as well as for the corrections to scaling, while Sec. IV focuses on the comparison between the NALF and the PALF. Section V gives a discussion and a summary of our findings. Details of the simulation algorithm and the parameters used are given in Appendixes A and B.

II. THEORETICAL RESULTS

A. Node-avoiding Lévy flight

In the segment (4) of d,μ space, the renormalization-group results[7,9] for the long-range n-vector model ferromagnet should apply for the NALF with $n \to 0$. The prediction for the end-to-end distance is of the form

$$\langle \ln R_N \rangle = \nu \ln[N(\ln N)^{\theta/\nu}] + \ldots , \tag{7}$$

where

$$\nu=1/\mu, \quad \theta=1/(4\mu) \quad (d=2\mu, \ 1 \le d < 4) . \tag{8}$$

For the segment (6) with $\mu > 2$, 2 should be substituted for μ in Eq. (8).

For the NALF in the segment of (5), the same approach can be extended very easily, since the relevant fixed points are the Gaussian long-range and short-range ones. Thus, in region I of Fig. 1, the relevant corrections to scaling exponents are

$$\Delta_1=(d-2\mu)/\mu, \quad \Delta_2=(2-\mu)/\mu , \tag{9}$$

where Δ_1 is associated with the quartic (or excluded-volume) term in the corresponding spin-model Hamiltonian, while Δ_2 is associated with the term k^μ, which gives rise to a long-range propagator. From these and the leading relevant exponent values of $\nu=1/\mu$ in region I and $\nu=\frac{1}{2}$ in region III, we find that

$$\nu=1/2, \quad \theta=1/2 \quad (d>4, \ \mu=2) . \tag{10}$$

This logarithmic power $\frac{1}{2}$ is in good agreement with the exact calculation of Hughes *et al.*[8] for the nonexcluded-volume Lévy flight at $\mu=2$ in arbitrary dimensions.

Along the boundary between regions II and IV, the corrections to scaling have not been evaluated theoretically, since the expansions of the exponents in powers of $\epsilon' \equiv 2-\eta_{\text{SR}}-\mu$, the distance from the boundary (SR refers to "short range"), are not available. However, expansions in powers of $\epsilon \equiv 2\mu-d$ from the boundary between regions I and II are available[7,9] and the correction exponent in this expansion associated with the long-range term (k^μ) is found to have a prefactor proportional to ϵ'. If we assume that this expansion can be applied at the boundary in question (between regions II and IV), the correction exponent would vanish there and introduce a multiplicative logarithmic correction.

Thus, along the boundaries of Eqs. (4) and (6), the logarithmic corrections are due to the excluded-volume term in the n-vector Hamiltonian, while along the boundary of Eq. (5) and that between regions II and IV, they are due to the long-range propagator term. Note that a confluence of these logarithmic corrections occurs at points $d=4$ and $\mu=2$. Because these are essentially orthogonal corrections, we expect the net result at the in-

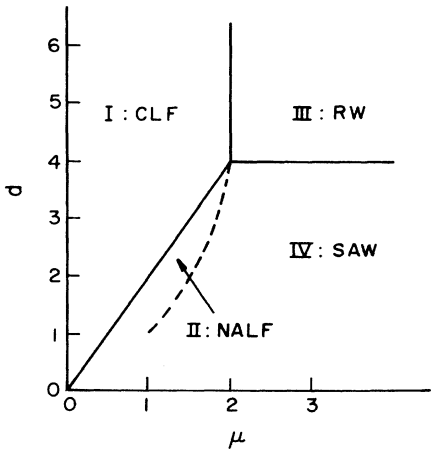

FIG. 1. Phase diagram in d,μ space for the node-avoiding Lévy flight. Four different regimes are shown: I, classical Lévy flight (CLF); II, node-avoiding Lévy flight (NALF); III, random walk (RW); IV, self-avoiding walk (SAW).

tersection to be additive. Accordingly we may expect a singular change in the apparent correction power observed in a numerical result at $d=4$, $\mu=2$. This is the first case of such confluence in critical phenomena that we are aware of.

We are also interested in the asymptotic behavior of the attrition rate characterized by the exponent γ. When there is a logarithmic correction to the asymptotic behavior Eq. (3), the weighted total number of walks is expected to be modified so that

$$\langle G_N \rangle = z_{\text{eff}}^N N^{\gamma-1} (\ln N)^{\phi} + \ldots . \tag{11}$$

For NALF at (4), the ϵ expansion by renormalization group for the exponent γ is known,[7,9] and the excluded-volume correction-to-scaling exponent can be shown to have the first-order term in ϵ equal to ϵ/μ. From this we see that

$$\gamma=1, \quad \phi=\tfrac{1}{4} \quad (d=2\mu, \ 1\le d<4) , \tag{12}$$

all along (4). Similarly, at the boundary of (5), the Gaussian predictions are

$$\gamma=1, \quad \phi=0 \quad (d>4, \ \mu=2) , \tag{13}$$

i.e., no logarithmic correction there. A logarithmic term with $\phi=\frac{1}{4}$ is expected for the segment (6) ($d=4$, $\mu>2$) from the known SAW results as well.

B. Path-avoiding Lévy flight

The theoretical situation for the PALF is much less clear. In one dimension, the PALF is essentially exactly solved[4,10] because of its simplicity unique to $d=1$. Thus for $d=1$, the values of ν are

$$\nu=1/\mu \quad (d=1, \mu\le 1) \tag{14}$$

and

$$\nu=1 \quad (d=1, \ \mu>1) , \tag{15}$$

with a logarithmic correction of $\theta=1$ only at $\mu=1$. The value of γ is always 1 because there is no attrition once a direction is determined; there is no logarithmic correction there, i.e., $\phi=0$.

However, for any higher d, very little can be stated. Here we first give a crude Flory-type argument[11] for the upper marginal dimensions and then describe an equivalent n-vector model Hamiltonian due to Woods Halley.[12]

Flory-type arguments have been given for the NALF previously,[1,3,13] which showed the upper marginal dimensions to be $d_c=2\mu$, in agreement with the renormalization-group theories.[7,9] In such arguments, the Flory free energy is estimated as the sum of the interaction part F_{int} and the entropic (or elastic) part F_{el}. For the NALF, F_{int} is taken to be N^2/R^d and F_{el} is taken as $(R^{\mu}/N)^x$, where $x=1$ or $x=1/(\mu-1)$ depending on the theory.[13] For the PALF, F_{el} is presumably unchanged but F_{int} should be changed to

$$F_{\text{int}} \propto N^{2y}/R^d , \tag{16}$$

where y is taken to be the one-dimensional PALF exponent ν because the excluded-volume effect should arise from all monomers along the chain.

In this crude argument, the upper marginal dimensions can be obtained by substituting the classical result $R=N^{1/\mu}$ in (16), and locating the boundary where the resulting F_{int} is asymptotically small. Here this gives

$$2y-d_c/\mu=0 , \tag{17}$$

and with Eqs. (14) and (15), this gives

$$d_c=2\mu \quad (\mu\ge 1) , \tag{18}$$

but

$$d_c=2 \quad (\mu<1) . \tag{19}$$

This is consistent with the absence of logarithmic corrections in $d=1$ the PALF at $\mu=\frac{1}{2}$ for example. While we could calculate ν in this approximation, such values are much less trustworthy. Also, since this discussion focuses on the exponent ν only, it really does not contain enough information on other exponents such as γ.

Now we describe an exact mapping[12] to an n-vector spin Hamiltonian in a way very similar to the NALF, in the hope that this would stimulate interest and eventually an analytic solution would be found. Thus the appropriate Hamiltonian for a hypercubic lattice is

$$-\beta H=\sum_{[i,j]} K_{ij} \prod_{\langle l,m\rangle\in\overline{(i,j)}} (\mathbf{s}_l\cdot\mathbf{s}_m) , \tag{20}$$

where the sum is over all pairs of sites separated in one of the coordinate directions, the product is over all nearest-neighbor pairs within the line segment from site i to j, and

$$K_{ij}=K_0/r_{ij}^{d+\mu} . \tag{21}$$

As usual, $\mathbf{s}$ is an n-component classical spin of length $\sqrt{n}$, and the limit $n\to 0$ is to be taken after the calculation of the correlation function, critical exponents, etc. The basic correspondence is between the two-point correlation function of (20) and the PALF generating function in the same manner as for the NALF or the SAW.[1]

III. MONTE CARLO SIMULATION

We performed Monte Carlo simulations of both the NALF and the PALF on hypercubic lattices for a set of points (d,μ)-parameter space lying along the boundaries of regions I and II, I and III, and III and IV in Fig. 1 with $d=2,3,4,5,6$ and $\mu=1,1.5,2.0,2.5,3.0$. Each walk consists of up to 400 steps and for each (d,μ) we obtained 80 000 to 460 000 400-step walks in total, which are generated in batches of the same size. Although the attrition due to the self-avoiding constraints in these dimensions is much less than in one dimension, the cumulative attrition rate for 400 steps turns out to be still enormous and the use of an enrichment technique[14] is essential for keeping computing time reasonable. Only some of the high-dimensional PALF could have been simulated in reasonable numbers without the use of enrichments. Details about the attrition rate and the enrichment parameters along with the computing time are discussed in Appendix A.

In one dimension,[4] the PALF's are relatively simple because each segment of the walk is extended in the same direction with no overlaps, while the NALF's are, in general, complex with many overlaps. In higher dimensions, however, the PALF is algorithmically more complex than the NALF due to the stricter constraint. The way to check for path avoidance is first to check whether the newly made segment and each of the previous ones form a two-dimensional plane or both lie on a straight line; then if either is the case, to pick those subspaces out of the hypercubic lattice and finally to check if the two line segments intersect each other. We will discuss more about this algorithm later in Appendix B.

Each individual step is completely specified by two random numbers, one for the step size, the other for the direction along the orthogonal coordinate axes. Given a random number r between 0 and 1, the step size can be assigned according to relation $dr=P(l)dl$, where $P(l)$ is Eq. (1) with a normalizing factor μ, that is,

$$P(l)=\mu l^{-\mu-1} ; \tag{22}$$

hence

$$l=(1-r)^{-1/\mu} , \tag{23}$$

and then l is replaced by a nearest integer since we are constrained to a discrete lattice. The directions are chosen randomly along one of the coordinate axes.

To investigate the exponent ν and the corrections to scaling, we define the effective exponent ν_N,[13]

$$\nu_N=\frac{N\exp(\langle \ln R_N\rangle)}{\frac{1}{2}[\exp(\langle \ln R_1\rangle)+\exp(\langle R_N\rangle)]+\sum_{i=2}^{N-1}\exp(\langle \ln R_i\rangle)}-1 . \tag{24}$$

The asymptotic behavior of ν_N for large N is then

$$\nu_N=\nu+\frac{\theta}{\ln N}+\frac{\theta}{(\nu+1)(\ln N)^2}+\ldots , \tag{25}$$

if there is a logarithmic correction, or

$$\nu_N=\nu+CN^{-\Delta}+\frac{C^2}{\Delta}N^{-2\Delta}+>\ldots , \tag{26}$$

if the correction is a power law (and $0<\Delta<\frac{1}{2}$).

Figure 2 shows the effective exponents from our Monte Carlo simulation of the NALF computed from the definition, Eq. (24), where the error bars indicate the standard deviations among 8–16 different batches of the same size for each (d,μ). To fit for the ν_N, however, Eqs. (25) or (26) could not be directly used with our data. In fact, an effective exponent defined in this way is convenient to see if a fit is good or not, but it is, in general, not suitable for computing the fit from, unless N is so large that the first two terms in these equations are sufficient by themselves.

Even though it is for this reason unfeasible to independently and accurately extract from our data the predicted exponents of the renormalization-group theory, it is possible to see how well those predictions agree with our Monte Carlo data. To do this we use the behavior of $\langle \ln R_N\rangle$ (Fig. 3) for fitting the coefficients in the general form of Eq. (7):

$$\exp(\langle \ln R_N\rangle)\approx N^{\nu}[A(\ln N)^{\theta}+B+CN^{-\Delta}+\ldots] , \tag{27}$$

if either $\Delta_1=0$ or $\Delta_2=0$, or

$$\exp(\langle \ln R_N\rangle)\approx N^{\nu}[A_1(\ln N)^{\theta_1}+A_2(\ln N)^{\theta_2}+B+\ldots] , \tag{28}$$

if $\Delta_1=\Delta_2=0$. The least-squares fits to these are calculated using the predicted values of the exponents such as Eqs. (8) and (10). We then compute what ν_N would be with these exponents and the fitted coefficients using Eq. (24), with N being treated as a continuous variable, i.e., the denominator of the equation being approximated as

$$\int_1^N \exp(\langle \ln R_x\rangle)dx .$$

This last step yields an excellent test of whether the fits are good because the effective exponents are very sensitive to the corrections to scaling.

The following is our result of fitting the coefficients in the above equations:

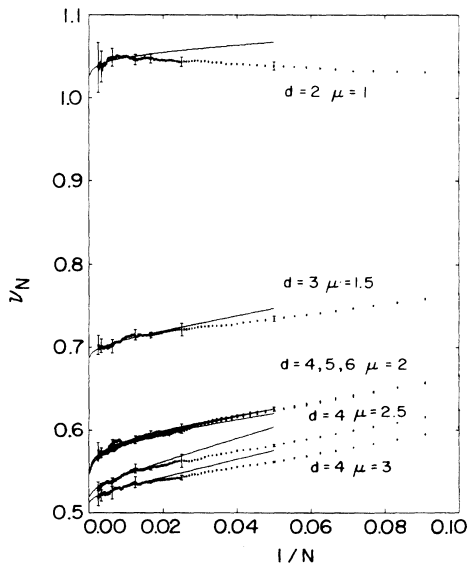

FIG. 2. Effective exponent ν_N defined by Eq. (24) and calculated from our Monte Carlo simulation of the NALF. The solid curves are from the best-fitted coefficients in Eq. (28) for $d=4$, $\mu=2$, and Eq. (27) for the rest. Error bars are the standard deviation among 8–16 batches of the same size for each d,μ.

$$\exp(\langle \ln R_N \rangle)$$

$$\approx N[1.596(\ln N)^{1/4}+0.400+0.575N^{-1}] \quad \text{for } d=2,\ \mu=1\ ,$$

$$\approx N^{2/3}[1.941(\ln N)^{1/6}-0.082+0.052N^{-1/3}] \quad \text{for } d=3,\ \mu=1.5\ ,$$

$$\approx N^{1/2}[1.295(\ln N)^{1/2}-2.946(\ln N)^{1/8}+3.454] \quad \text{for } d=4,\ \mu=2\ ,$$

$$\approx N^{1/2}[1.984(\ln N)^{1/8}-0.443-0.296N^{-1}] \quad \text{for } d=4,\ \mu=2.5\ ,$$

$$\approx N^{1/2}[1.090(\ln N)^{1/8}+0.335-0.225N^{-1}] \quad \text{for } d=4,\ \mu=3\ ,$$

$$\approx N^{1/2}[0.932(\ln N)^{1/2}+0.608+0.407N^{-1/2}] \quad \text{for } d=5,\ \mu=2\ ,$$

$$\approx N^{1/2}[0.849(\ln N)^{1/2}+0.823+0.447N^{-1}] \quad \text{for } d=6,\ \mu=2\ .$$

The range of N for the fit is $N=10$–400, except for $d=2$, $\mu=1$, for which N was taken to be from 20 to 400. Although the errors of these fits are within 5% (mostly less than 1%), the fitted coefficients vary sensitively if the range of N is changed (as in most cases of multivariable fits). Thus our result is somewhat subjective in that the coefficients are selected only because they give the best visual fit in Fig. 2 for the given exponents (Fig. 2 compares our direct Monte Carlo result for ν_N with the fits so obtained).

We can also clearly see from Figs. 2 and 3 that $d=4$ is the upper marginal dimension for $\mu=2$. The ν_N for $d=1$, $\mu=2$ in the previous work[4] were all greater than 1.0 (data were obtained for up to the hundreth step) and we obtained one or two batches of data for $d=2,3$ with $\mu=2$ to verify that the asymptotic behavior of ν_N gradually collapses down to that of $d=4$, $\mu=2$.

The Monte Carlo result for ν_N of the PALF (Fig. 4) with the same parameters (d,μ) is quite similar to that of the NALF for $d\geq 4$. In spite of the absence of theoretical predictions such as Eqs. (27) or (28), we attempted to fit the data with Eqs. (27) and (28), using the same method as for the NALF. We could obtain reasonably good fits that way, although the fitted values of the coefficients are different from those of the NALF and the asymptotic behavior of ν_N for $d=2,3$ is noticeably different from the NALF. However, since our simulation is limited to a relatively small number of steps and since some direct comparisons between the two self-avoiding Lévy flights show clear differences as discussed in Sec. IV, we reserve our judgment on whether their critical exponents and corrections to scaling are the same at $d=2\mu$, in general.

For the estimation of exponent γ we first note that the probability p_N that a self-avoiding Lévy flight can survive, the self-avoiding constraints after N steps, may be defined as

$$p_N \equiv \frac{G_N}{G_N^{\mathrm{RW}}}\ , \tag{29}$$

where G_N^{RW} is the number of N-step random walks, which is z^N if the coordination number of the lattice in question is z. This definition is equivalent to Eq. (1) of Ref. 13 without the logarithmic correction factor. p_N can also be

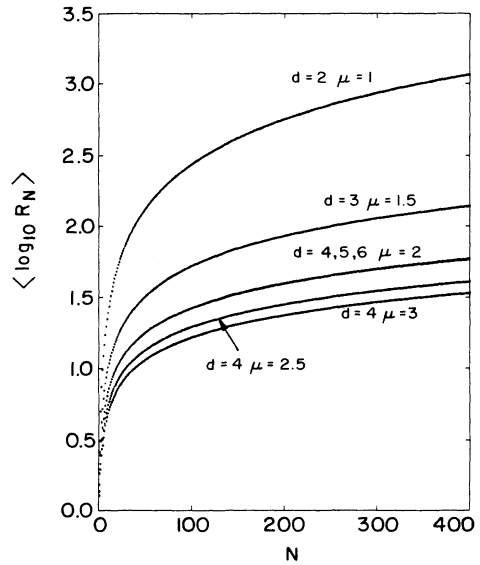

FIG. 3. Logarithmic moment of the end-to-end distance of the NALF. Data points for $d=4,5,6$, $\mu=2$ seem to be on top of one another in the scale used, which is a strong indication that $d=4$ is the upper marginal dimension for the self-avoiding Lévy flights. See also Figs. 1 and 2 for this point.

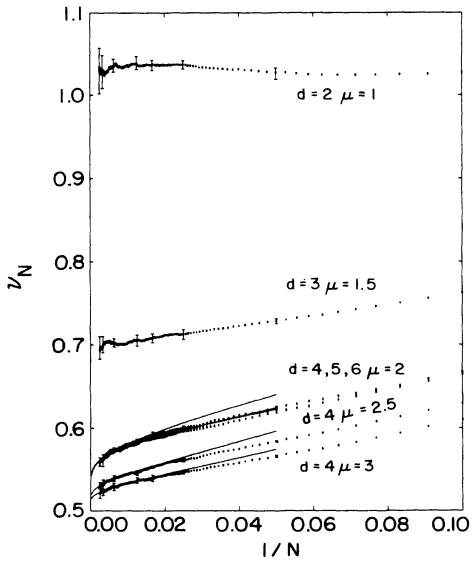

FIG. 4. Effective exponent ν_N defined by Eq. (24) and calculated from our Monte Carlo simulation of the PALF. The fitting curves were obtained in the same way as for the NALF and shown for $d\geq 4$ where both types of Lévy flight are expected to be in the same universality class.

defined algorithmically as

$$p_N \equiv \lim_{A_1 \to \infty} \frac{A_N}{A_1} , \tag{30}$$

where A_i is the number of successful i-step walks obtained from the computer simulation.

Now let us define the local survivability S_N of the Nth step:

$$S_N \equiv \lim_{A_1 \to \infty} \frac{A_N}{A_{N-1}} = \frac{p_N}{p_{N-1}}, \quad S_1 = 1 . \tag{31}$$

The logarithm of S_N shows an asymptotic behavior

$$\ln S_N \approx \ln \frac{z_{\text{eff}}}{z} + (\gamma - 1)\frac{1}{N} + \frac{\phi}{N \ln N} + O\left[\frac{1}{N^2}\right] \tag{32}$$

for large N. Thus one can estimate the values of γ, ϕ, and z_{eff} from the $\ln S_N$ versus $1/N$ plot (Fig. 5). Table I shows the values of γ and z_{eff} along the three segments of (d,μ) space estimated by use of the least-squares fit, without the logarithmic correction term, taking the data for $N = 20$–400.

We also tried fitting for ϕ for $d = 2,3,4$ in various ways. Fixing $\phi = \frac{1}{4}$ always produces an underestimation of γ by an amount comparable to the overestimation made from the simple nonlogarithmic fitting. The errors of γ in Table I are the deviation of γ obtained this way from the known classical value (which is 1). On the other hand, fixing $\gamma = 1$ or fitting for both γ and ϕ as free parameters give much smaller ϕ than the theoretical prediction (mostly, between 0.03 and 0.13). However, z_{eff} seems to vary little in any case and the fit error is less than 0.1%.

We especially note that γ for the PALF for $d = 2$, $\mu = 1$ suggests a short-range behavior. This value

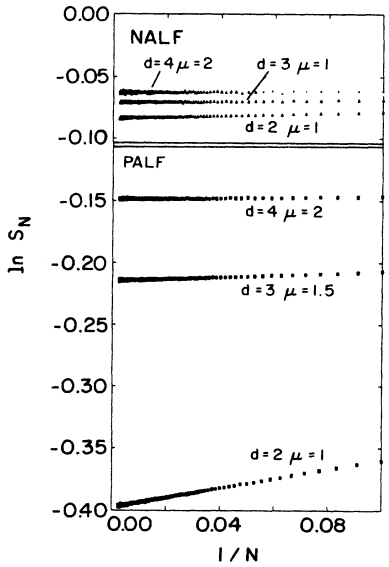

FIG. 5. Logarithm of the local survivability as defined in Eq. (31), plotted against $1/N$. The slope at $1/N \to 0$ gives $\gamma - 1$ and $S_N \to z_{\text{eff}}/z$ as $N \to \infty$. See Eq. (32) and Table I for details.

TABLE I. Exponent γ and the ratio z_{eff}/z for the NALF and the PALF. The γ were obtained from the least-squares fit without logarithmic correction. For the NALF in $d = 2,3,4$ and the PALF in $d = 4$, where the logarithmic correction $\phi = \frac{1}{4}$ is expected, the error indicates the underestimation of γ from its classical value 1 obtained from a fit including the logarithmic term with $\phi = \frac{1}{4}$ fixed. The error for z_{eff}/z is less than 0.1% for all d. Data were taken for $N = 20$–400.

	NALF		PALF	
(d,μ)	γ	z_{eff}/z	γ	z_{eff}/z
$d=2$, $\mu=1$	1.05±0.03	0.92	1.38±0.00	0.67
$d=3$, $\mu=1.5$	1.02±0.06	0.93	1.07±0.00	0.81
$d=4$, $\mu=2$	1.01±0.07	0.94	1.01±0.06	0.86
$d=4$, $\mu=2.5$	1.02±0.06	0.93	1.02±0.05	0.86
$d=4$, $\mu=3$	1.02±0.06	0.91	1.03±0.05	0.86
$d=5$, $\mu=2$	1.00±0.00	0.95	0.99±0.03	0.89
$d=6$, $\mu=2$	1.00±0.00	0.96	1.00±0.00	0.91

is to be compared with the SAW values[14] of γ of approximately $\frac{4}{3}$ in two dimensions. This is a strong indication that at least at $d = 2$, $\mu = 1$, the PALF is not classical and quite different from the NALF.

IV. COMPARISONS BETWEEN THE NALF AND THE PALF

One surprising result of the one-dimensional self-avoiding Lévy flight is that the end-to-end distance of the NALF is greater than that of the PALF, even if the backtracking is allowed for the NALF, while the PALF never turns back once the direction is initially chosen.

We find that this is no longer true for all upper marginal dimensions greater than 1. On the contrary, the end-to-end distance of the PALF is always greater than that of the NALF, if not by far, while the individual step sizes of the NALF are still larger than those of the PALF. This is not very straightforward. One possible explanation is as follows. As the dimension becomes higher, the node-avoiding constraint is more rapidly loosened than the path-avoiding one. Thus the tendency of the NALF to *step aside* from a previously occupied site is more easily neutralized by the easier backtracking in higher dimensions than the tendency of the PALF to spread out to avoid intersections altogether, right from $d = 2$. But as far as an individual step is concerned, it is intuitively plausible that the longer the step the more difficult it is to survive the path-avoiding constraints rather than the node-avoiding ones; hence the larger steps for the NALF.

Figure 6 shows the comparisons for both the zeroth moment of end-to-end distance (below the ratio 1) and the individual step sizes (above the ratio 1). Another interesting feature observed from this figure is that the end-to-end distances of the NALF and the PALF are very close to each other (within 1%) while their individual step sizes are quite different, most prominently in $d = 2$ (by 15%). Beyond $d = 2$, however, the difference in individual step sizes drastically drops down to about 5% and the ratio slowly approaches 1 as d increases.

We are also interested in the question: Is the step-size

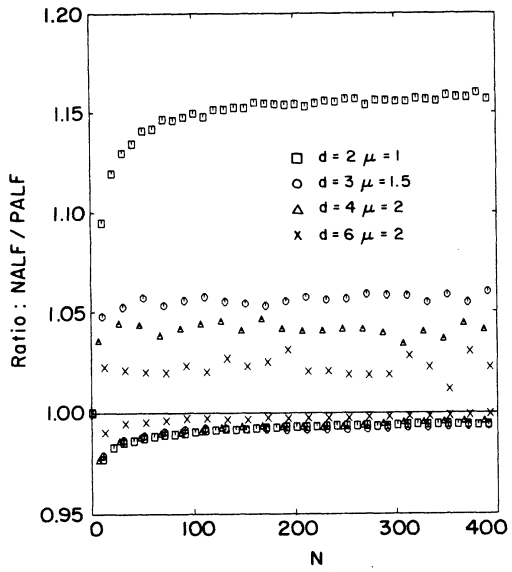

FIG. 6. Direct comparisons between node-avoiding and path-avoiding Lévy flights. The points in the upper part of the diagram show the ratios of the individual step sizes and those in the lower part show the ratios of the end-to-end distances.

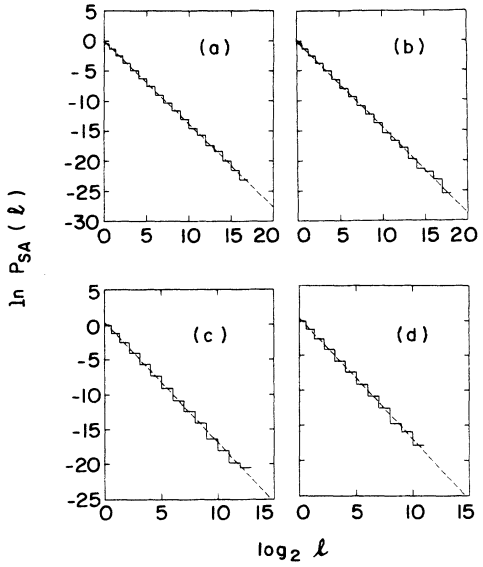

FIG. 7. Some typical examples of the actual step-size distribution for the NALF and the PALF. Natural logarithm is used in the ordinate while the logarithm with base 2 is used in the abscissa for convenience. If the step-size distribution of the self-avoiding Lévy flights is still a power law, then the slope of these plots gives $-(\mu_{\rm eff}+1)\ln 2$ [Eq. (33)]. (a) NALF; $d=2$, $\mu=1$; 360th step; $\mu_{\rm eff}=0.999\pm0.001$. (b) PALF; $d=2$, $\mu=1$, 361st step; $\mu_{\rm eff}=1.076\pm0.01$. (c) NALF; $d=3$, $\mu=1.5$; 360th step; $\mu_{\rm eff}=1.483\pm0.002$. (d) PALF; $d=3$, $\mu=1.5$; 361st step; $\mu_{\rm eff}=1.493\pm0.002$.

distribution of both types of self-avoiding Lévy flights still a power law? If this is the case, what is the effective Lévy index that characterizes the distribution? To see this we collect the surviving steps for every 20th step of both the NALF and the PALF in $d=2,3$ and plot the size distribution in log-log scale. The individual step sizes are categorized by the range into which they fall, which is delimited by integer powers of 2. If the actual size distribution of the self-avoiding Lévy flights is still a power law, that is, $P_{\rm SA}(l)\propto l^{-1-\mu_{\rm eff}}$, then the slope of the log-log plot is related to the $\mu_{\rm eff}$ by

$$\ln P_{\rm SA}(l)=-(\mu_{\rm eff}+1)(\ln 2)\log_2 l+\text{const} . \qquad (33)$$

One might expect that the NALF for $d=2\mu$ would have the power-law distribution, since the parameters (d,μ) for those are at the boundary of the classical Lévy flight region. Our data strongly suggest that this is indeed true for *both* the NALF and the PALF. This is all the more remarkable because even at the upper marginal dimensions, the attrition for these Lévy flights is enormous at $N\gtrsim 300$, unlike the classical Lévy flights which, of course, have no attrition at all. Some typical examples of the actual size distributions are presented in Fig. 7 where the log-log scale is used with different bases for convenience.

The values of $\mu_{\rm eff}$ are also computed through the least-squares fit: For $d=2$, the $\mu_{\rm eff}$ of the NALF do not differ from the original μ $(=1)$ by more than 2%, but those of the PALF are 6–8 % larger, and for $d=3$, $\mu_{\rm eff}$ becomes even closer to μ $(=1.5)$ for both cases. It should be noted that the PALF's always have greater $\mu_{\rm eff}$ than NALF, which is consistent with the direct comparison of the individual step sizes.

The question of how this $\mu_{\rm eff}$ is related to other properties of the self-avoiding Lévy flights seems to remain open at this time. If the actual step size were distributed *exactly* as a power law with $\mu_{\rm eff}$, then the logarithmic moment of a single step size would be simply equal to $1/\mu_{\rm eff}$; however, the power law is asymptotic at best, and also our use of discrete lattice gets in the way of this type of identification. While there appears to be asymptotic self-similarity in step-size distribution with the dimensionality of $\mu_{\rm eff}$, again it is unclear whether this should be identical to the self-similarity in overall *conformation* of the chain (whose *fractal* dimension should be $1/\nu$).

V. SUMMARY AND DISCUSSION

We have numerically tested the predictions of the renormalization-group theory for the critical exponents of the NALF, including the corrections to scaling, and obtained a consistent result for all upper marginal dimensions of the NALF. The PALF seems to be different from the NALF, especially in two dimensions where it shows a short-range behavior for γ while the NALF does not appear to, and the asymptotic behavior of ν_N is apparently different from that of the NALF. This may raise a question that $d=2\mu$, $\mu\leq 2$ might not be the right boundary of the classical and excluded-volume regions of the Lévy flight with path-avoiding constraints. Nevertheless, for $d\geq 4$, $\mu\geq 2$ our numerical result presents a manifestation that the NALF and the PALF are of the

same universality class.

The direct comparison between the two self-avoiding Lévy flights shows an interesting feature that the end-to-end distance of the PALF is larger than that of the NALF, contrary to the one-dimensional results, while the individual step size is always smaller.

We have also shown that the actual step-size distribution of the two types of self-avoiding Lévy flights is still a good power law characterized by an effective Lévy index, which is qualitatively consistent with the direct comparison for the individual step sizes. These points again suggest, as usual, that the global property of a non-Markovian random walk depends in a complicated way on the property of individual steps and the nature of global constraints.

ACKNOWLEDGMENTS

We thank J. Woods Halley for discussions and encouragement and are also grateful to the Donors of the Petroleum Research Fund administered by the American Chemical Society for partial support of this work.

APPENDIX A: MONTE CARLO METHOD

In this appendix we present some details of our simulations described in Sec. III. The existence of a certain maximum step size that can be generated by a computer is an inescapable limitation of simulations of this kind. In particular, each individual step of the Lévy flight has infinite mean step size if $\mu \leq 1$, which is impossible to realize by computer simulations. This is in fact the reason why we take the zeroth moment of the end-to-end distance $\langle \ln R_N \rangle$, which is always finite no matter what μ. The limitations on the maximum step sizes, the random number generations, and the truncation errors were discussed in detail in the previous paper on the one-dimensional Lévy flights.[4]

In higher dimensions, the attrition due to the self-avoiding constraints turns out to be still high, so that we need to use an enrichment technique. For instance, in two dimensions, each new step of the NALF survives the self-avoiding constraint with a probability of 92%, which means that roughly $1/0.92^{400} \approx 10^{15}$ random numbers should have been generated to obtain a single walk of 400 steps if enrichment were not used.

The parameters for a standard enrichment technique[12] used in our Monte Carlo simulations of the NALF and the PALF are shown in Tables II and III, respectively. We used machines with 32-bit Fortran integers (ISI 68020 V24, DEC VAX 11/750, GOULD PN9080, GOULD NP-1, and CCI 6/32 computers) for most of the simulations and a machine with 48-bit Fortran integers (Control Data Corporation Cyber 205 computer) for the major part of the NALF in $d=2,3$. The computing time of the simulations varies from machine to machine and also depends on the enrichment parameters as well as d and μ. The average CPU time to generate one successful 400-step walk with the 32-bit machines used was roughly at least 10 sec for most of the d,μ and we consumed over 4000 CPU h to get our simulation data from these machines. On the other hand, the Cyber 205 super computer took about 1 sec to generate one 400-step NALF with $d=2$, $\mu=1$ and 1.5 sec for one with $d=3$, $\mu=1.5$ using appropriate enrichment parameters, and the total CPU time on this machine was at least 16 h.

APPENDIX B: THE PALF ALGORITHM

We discuss here the loop-checking routine of the PALF algorithm in more detail. Checking the node avoidance is relatively simple because it is sufficient to store only the end-point positions of the previous steps to compare with the position of the currently attempted step. For the *path* avoidance, however, all the lattice sites between the successive end points, that is, the whole segment of each step, should be taken care of. But our algorithm checks this by keeping track of only the end-point coordinates and the direction of each segment without having to store every lattice site that the segments contain.

Suppose we make steps in a d-dimensional hypercubic lattice starting at the origin. Each step is viewed as a segment connecting the starting and the ending points and can be represented by a vector along one of the orthogonal axes, that is, for the ith segment,

$$\mathbf{l}^{(i)} = l^{(i)} \hat{\mathbf{e}}_{k_i}, \quad i = 1, 2, \ldots,$$

TABLE II. The parameters used in the Monte Carlo simulations of the node-avoiding Lévy flights. The number of walks generated is indicated at the first and last steps, and the number of stages, length of each stage, and the number of allowed trials per stage refer to the parameters of a standard enrichment technique.

(d,μ)	Number of stages	Length of stage	Number of trials per stage	Number of walks First step	Number of walks Last step
$d=2$, $\mu=1.0$	20	20	5	6 412 075	461 066
$d=3$, $\mu=1.5$	40	10	17[a]	6 458 357	320 960
$d=4$, $\mu=2.0$	40	10	12	1 764 300	120 622
$d=4$, $\mu=2.5$	40	10	21[a]	2 214 227	80 155
$d=4$, $\mu=3.0$	40	10	35[a]	3 445 332	79 923
$d=5$, $\mu=2.0$	50	8	10	1 163 170	80 029
$d=6$, $\mu=2.0$	50	8	6	1 033 014	78 465

[a]Slightly different numbers were also tried for some batches.

TABLE III. The parameters used in the Monte Carlo simulations of the path-avoiding Lévy flights. The number of walks generated is indicated at the first and last steps, and the number of stages, length of each stage, and the number of allowed trials per stage refer to the parameters of a standard enrichment technique.

(d,μ)	Number of stages	Length of stage	Number of trials per stage	Number of walks First step	Number of walks Last step
$d=2,\ \mu=1.0$	20	20	8[a]	3 740 140	254 114
$d=3,\ \mu=1.5$[b]	100	4	21	3 381 457	155 395
$d=4,\ \mu=2.0$	100	4	4	613 800	98 588
$d=4,\ \mu=2.5$	100	4	5	692 685	80 006
$d=4,\ \mu=3.0$	100	4	7[a]	643 268	80 007
$d=5,\ \mu=2.0$	200	2	4[a]	434 326	80 119
$d=6,\ \mu=2.0$	200	2	2	279 224	80 403

[a]Slightly different numbers were also tried for some batches.
[b]A different set of parameters (50,8,5) was used for the first 5 out of 15 batches.

where $\hat{\mathbf{e}}_{k_i}$ is the unit vector along the k_ith coordinate axis, k_i taking on one of the integers from 1 to d. The absolute value of $l^{(i)}$ is determined by a random number, as explained in Sec. III with Eq. (23), and the sign of $l^{(i)}$ and k_i by another random number. The position of the walker after making N steps can also be represented by a vector,

$$\mathbf{X}^{(N)}=(X_1^{(N)},X_2^{(N)},\ldots,X_d^{(N)}) ,$$

where $\mathbf{X}^{(0)}$ is the origin and

$$X_k^{(N)}=\sum_{i=1}^{N}\mathbf{l}^{(i)}\cdot\hat{\mathbf{e}}_k,\quad k=1,2,\ldots,d .$$

Note that $\mathbf{l}^{(i)}$ starts at $\mathbf{X}^{(i-1)}$ ending at $\mathbf{X}^{(i)}$, thus

$$\mathbf{X}^{(i)}=\mathbf{X}^{(i-1)}+\mathbf{l}^{(i)} ,$$

that is,

$$X_{k_i}^{(i)}=X_{k_i}^{(i-1)}+l^{(i)} ,$$

$$X_k^{(i)}=X_k^{(i-1)}\ \text{ for all } k\neq k_i .$$

In the actual program, we keep two separate arrays to store the values of $l^{(i)}$ and k_i in addition to an array for $X_k^{(i)}$ for all i and k.

Now suppose that we are about to make an Nth step after $N-1$ successful steps. We generate $\mathbf{l}^{(N)}$ and wish to check if this new segment crosses any of the previous segments. Let us take, say, the ith segment, $\mathbf{l}^{(i)}$ and check for this condition. A necessary condition for intersection is that both $\mathbf{l}^{(i)}$ and $\mathbf{l}^{(N)}$ lie either in a two-dimensional subspace (a plane) if $k_i\neq k_N$ or on a straight line if $k_i=k_N$. This condition is easily checked to be true if

$$\sum_{k(\neq k_i,k_N)}|X_k^{(N)}-X_k^{(i)}|=0 ,$$

where the summation is over all coordinates 1 to d, except for k_i and K_N.

Now, if both $\mathbf{l}^{(i)}$ and $\mathbf{l}^{(N)}$ lie on a plane defined by $\hat{\mathbf{e}}_{k_i}$ and $\hat{\mathbf{e}}_{k_N}$, they cross if and only if

$$(X_{k_N}^{(N)}-X_{k_N}^{(i)})(X_{k_N}^{(N-1)}-X_{k_N}^{(i)})\leq 0$$

and

$$(X_{k_i}^{(i)}-X_{k_i}^{(N)})(X_{k_i}^{(i-1)}-X_{k_i}^{(N)})\leq 0 .$$

On the other hand, if the two segments lie on a straight line, that is, $k_i=k_N=n$, then they cross if and only if

$$\max\{X_n^{(i)},X_n^{(i-1)},X_n^{(N)},X_n^{(N-1)}\}$$

$$-\min\{X_n^{(i)},X_n^{(i-1)},X_n^{(N)},X_n^{(N-1)}\}\leq|l^{(i)}|+|l^{(N)}| .$$

The checking procedure is repeated for $i=1,\ldots,N-3$, and the Nth step is accepted if $\mathbf{l}^{(N)}$ is found to be path avoiding. Otherwise, the attempt is a failure and another walk is started either from the origin for simple sampling or from the end of the previous stage if the enrichment is being used.[14]

[1]J. W. Halley and H. Nakanishi, Phys. Rev. Lett. **55**, 551 (1985).
[2]B. B. Mandelbrot, *Fractals, Form, Chances and Dimensions* (Freeman, San Francisco, 1977); see also B. D. Hughes, M. F. Shlesinger, and E. W. Montroll, Proc. Natl. Acad. Sci. U.S.A. **78**, 3287 (1981) for the spatially discrete case.
[3]E. Bouchaud and M. Daoud, J. Phys. A **20**, 1463 (1987).
[4]S. B. Lee, H. Nakanishi, and B. Derrida, Phys. Rev. A **36**, 5059 (1987).
[5]J. J. Prentis and W. R. Geisler, J. Phys. A. **19**, L161 (1986).
[6]See, e.g., H. Eugene Stanley, *Introduction to Phase Transitions and Critical Phenomena* (Oxford University, New York, 1971); the first correspondence between the $n\rightarrow 0$ limit of the n-vector model and the statistics of the SAW is due to P. G. de Gennes, Phys. Lett. **38A**, 339 (1972).
[7]M. E. Fisher, S. K. Ma, and B. G. Nickel, Phys. Rev. Lett. **29**, 917 (1971); J. Sak, Phys. Rev. B **8**, 281 (1973).

[8]B. D. Hughes, E. W. Montroll, and M. F. Shlesinger, J. Stat. Phys. **28**, 111 (1982).
[9]J. J. Prentis, J. Phys. A. **18**, L833 (1985).
[10]S. Havlin, A. Bunde, and H. E. Stanley, Phys. Rev. B **34**, 1 (1986) gives a scaling argument for the PALF in one dimension.
[11]See, e.g., P. G. de Gennes, *Scaling Concepts in Polymer Physics* (Cornell University, Ithaca, NY, 1979).
[12]J. Woods Halley (private communication).
[13]P. Grassberger, J. Phys. A **18**, L463 (1986).
[14]F. T. Wall, S. Windwer, and P. J. Gans, Methods Comput. Phys. **1**, 217 (1963).